

# Power deposition by mode converted electron Bernstein waves in the DIII-D ‘heat pinch’ experiments

C.B. Forest

Department of Physics, University of Wisconsin,  
Madison, Wisconsin, United States of America

R.W. Harvey

CompX,  
Del Mar, California, United States of America

A.P. Smirnov

Moscow State University,  
Moscow, Russian Federation

**Abstract.** Mode converted electron Bernstein waves are shown to play an important role in power deposition in the off-axis electron cyclotron heating experiments on the DIII-D tokamak in which the effect known as the ‘heat pinch’ was inferred. Ray tracing shows that the mode converted Bernstein modes (generated when the launched X mode reflects from an outboard upper hybrid layer) are damped in the central region where the previous transport analysis had assumed no power was being deposited.

A transport analysis of off-axis electron cyclotron heating (ECH) of DIII-D tokamak plasmas showed a ‘heat pinch’ in which electron energy was transported inward, apparently flowing up the electron temperature gradient [1, 2]. From this, the authors drew the conclusion that the simple Fourier heat law  $q_e = -n\chi_e\nabla T_e$  could not be entirely responsible for electron energy transport in tokamaks, since the experiment would require a negative value of  $\chi_e$ . If there were a negative heat flux, this would also imply that non-linear diffusivities and critical temperature gradient models could not completely explain the cross-field transport in tokamak plasmas. The experiments suggested that the heat pinch increased with density. The power balance analysis used, and therefore the conclusions drawn from these experiments, depend critically on estimates of the power deposition profile of the heating. This article uses new functionality in the ray tracing code GENRAY, incorporating the full hot plasma ray tracing equations to calculate the power deposition profile. We find that inclusion of the hot plasma electron Bernstein wave (EBW) in the power absorption calculation results in significant power deposition in the central region that was not accounted for in the power balance analysis; thus the strength of the inferred heat pinch is greatly reduced, and the region over which inward heat flow

is implied is significantly smaller. This article does not attempt to re-evaluate the energy transport in these discharges, rather we attempt only to provide a complete power deposition calculation for a representative case.

The DIII-D ECH experiments used inside launch, X mode polarized electron cyclotron waves. Approximately 1 MW of power was launched from the inner wall of the tokamak at a frequency of 60 GHz, which is equal to the cyclotron frequency at a magnetic field of 2.14 T. In all the heat pinch experiments, off-axis heating was realized by adjusting the toroidal field strength such that the cyclotron resonance layer was located on the inboard side of the magnetic axis, as shown in Fig. 1. Thus the launched ECH power encounters a cyclotron resonance before it reaches the core.

For the parameters of the DIII-D experiments, the X mode has the property that only a fraction of the power is absorbed on the first pass of the microwave beam through the resonance. Indeed, the first pass absorption is expected from ECH theory to decrease as the density increases. Interestingly, the largest interpreted inward heat transport was observed in discharges for which the first pass absorption through the cyclotron layer was lowest (at the highest densities). Theory predicts that the fraction of power

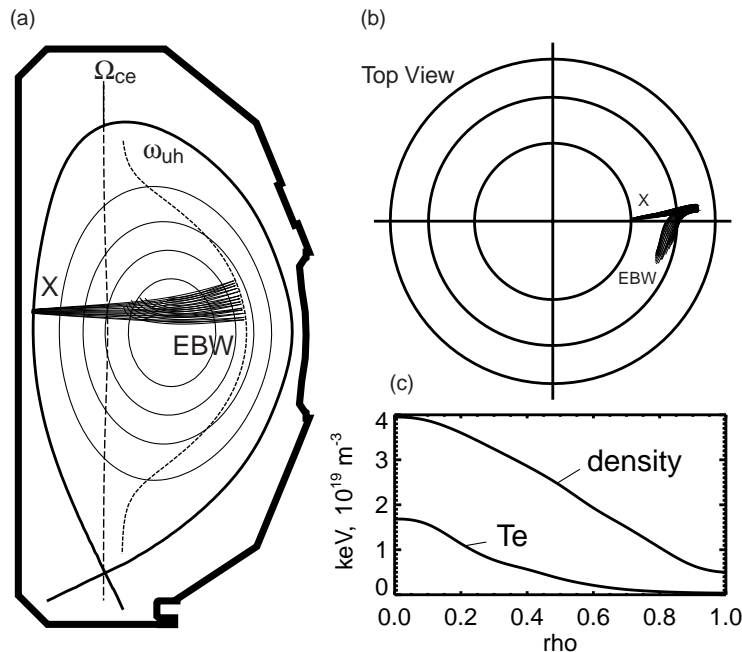


**Figure 1.** (a) Geometry for the DIII-D inside launch, 60 GHz, X mode heating system. The positions of the cyclotron resonance layer ( $\omega_{rf} = \Omega_{ce}(\mathbf{r})$ ) and the upper hybrid resonance layer ( $\omega_{uh}^2 = \Omega_{ce}^2 + \omega_{pe}^2$ ) are shown. The bundle of ray trajectories is used to model the launched X mode and the mode converted EBW. (b) Top view of the ray trajectories. (c) Temperature and density profiles used for the calculations in this article.

transmitted on the first pass is  $e^{-\tau_X}$ , where

$$\tau_X = \frac{\pi}{2} N^3 N_{\parallel}^2 \left( 1 + \frac{\omega_{pe}^2}{\Omega_{ce}^2} \right)^2 \frac{\Omega_{ce}^2}{\omega_{pe}^2} \frac{kT_e}{m_e c^2} \frac{cR}{\omega_{rf}} \quad (1)$$

is the optical thickness for obliquely launched X mode radiation [3]. Here  $\omega_{rf}$  is the frequency of the launched power,  $N$  is the index of refraction for the X mode and is of order 1,  $N_{\parallel} = ck_{\parallel}/\omega_{rf}$  is the component in the direction of the magnetic field,  $\Omega_{ce}$  is the local cyclotron frequency,  $\omega_{pe}$  is the local plasma frequency and  $R$  is the major radius at the resonance location. The optical thickness  $\tau_X$  is a monotonically decreasing function of density for fixed temperature  $T_e$ .

For these experiments this fraction varied from approximately 10% at low density ( $n_e(0) \approx 10^{13} \text{ cm}^{-3}$ ) to greater than 50% at high density ( $n_e(0) \approx 4 \times 10^{13} \text{ cm}^{-3}$ ). The transmitted power fraction  $e^{-\tau_X}$  is then expected to continue to propagate towards lower magnetic fields where it encounters the upper hybrid layer and is mode converted with nearly 100% efficiency into the EBW, which

propagates back towards the cyclotron resonance layer. The previous analysis used an ad hoc absorption model for this transmitted power in which the power returning from the upper hybrid region was distributed over the cold plasma cyclotron resonance layer with a spatial distribution proportional to the electron temperature. That model therefore precluded any power deposition inside the resonance layer where the X mode was depositing its power.

It is well known that the X mode is reflected from the upper hybrid layer in the form of an EBW, an electrostatic, hot plasma wave which propagates back towards the resonance layer. Indeed, this is the classic mode conversion problem and we refer interested readers to the original work by Stix [4] and to later work by Schuss and Hosea [5] where an elementary discussion of the mode conversion process is presented. The specific role of the EBW in the absorption processes was not accounted for in Ref. [1]. For the DIII-D heat pinch experiments, the upper hybrid layer associated with the densities studied is typically located on the low field side of the magnetic axis; increasing the density moves the upper hybrid

layer further away from the cyclotron resonance. This article is primarily concerned with the propagation and absorption of the mode converted EBW as the waves propagate from the upper hybrid layer towards the cyclotron resonance. We use the ray tracing code GENRAY, which treats the propagation and absorption of both the X mode and the EBW [6], to show that the remaining ECH power is deposited largely in the central region.

The dispersion (and therefore propagation and absorption) of the EBW is a complicated function of primarily the magnetic field strength and the electron temperature. Here the propagation and absorption of the EBW are studied numerically using the WKB approximation. The dispersion function used is a numerical implementation of the fully electromagnetic, hot plasma dielectric tensor [7]. The determinant of the Hermitian part of the dielectric tensor results in a dispersion function  $D[n_e(\mathbf{r}), B(\mathbf{r}), T_e(\mathbf{r}), N_\perp, N_\parallel, \omega_{rf}] = 0$ . For a given electron density  $n_e$ , magnetic field strength  $B$ , electron temperature  $T_e$  and  $N_\parallel = ck_\parallel/\omega_{rf}$  this equation can be solved to find  $N_\perp = ck_\perp/\omega_{rf}$ .

Once a dispersion function  $D$  is known, the ray equations are [7]

$$\frac{d\mathbf{r}}{dt} = V_{g,\perp} \frac{\mathbf{N} - N_\parallel \mathbf{b}}{N_\perp} + V_{g,\parallel} \mathbf{b} \quad (2a)$$

$$\frac{dN}{dt} = \frac{c}{\omega} \frac{\partial D / \partial \mathbf{r}}{\partial D / \partial \omega} \quad (2b)$$

where  $\mathbf{b}$  is a unit vector aligned with the magnetic field,  $\mathbf{N} = c\mathbf{k}/\omega$ ,  $N_\parallel = \mathbf{N} \cdot \mathbf{b}$  and

$$V_{g,\perp} = -\frac{c}{\omega} \frac{\partial D / \partial N_\perp}{\partial D / \partial \omega} \quad (3a)$$

$$V_{g,\parallel} = -\frac{c}{\omega} \frac{\partial D / \partial N_\parallel}{\partial D / \partial \omega}. \quad (3b)$$

The power absorption along a ray is related to the anti-Hermitian part of the dielectric tensor and requires special treatment to properly address the relativistic resonance condition.

The power of the EBW is absorbed by electrons satisfying the Doppler shifted cyclotron resonance condition:

$$N_\parallel \frac{v_\parallel}{c} + \frac{\Omega_{ce}(\mathbf{x})}{\gamma \omega_{rf}} = 1 \quad (4)$$

where  $\gamma$  is the usual relativistic factor. For the launched X mode we have  $k_\parallel v_{te}/\omega_{rf} \ll 1$ , where  $v_{te}$  is the thermal velocity of the electrons; thus

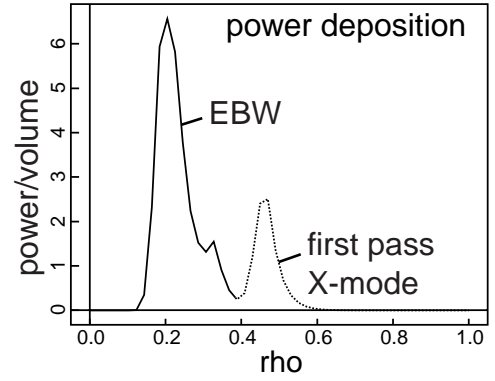


**Figure 2.** Calculated deposition profiles including the EBW. The deposition profiles are estimated by launching a bundle of 30 rays to represent the launched  $N_\parallel$  spectrum of the antenna. The equilibrium is representative of an  $I_p = 500$  kA,  $B_\phi = 1.7$  T discharge in DIII-D.

the power is absorbed where  $\Omega_{ce}(\mathbf{x}) \approx \omega_{rf}$  (shown in Fig. 1 for a particular DIII-D equilibrium). The power deposition of the EBW is also determined by the resonance condition in Eq. (4); however, the  $N_\parallel$  of the EBW varies with the toroidal geometry, and this plays a dominant role in determining the power deposition profile. For finite  $N_\parallel$  ( $\sim 1$ ), the power can be absorbed at a point shifted by an amount

$$\Delta R \approx 3N_\parallel \frac{v_{te}}{c} R$$

which is found to be tens of centimetres for the DIII-D case.

Power deposition profiles that include the mode converted EBW are shown in Fig. 2. The temperature profile is shown in Fig. 1(c) and is representative of the temperature profile after the ECH is turned on and after transport equilibrium is reached (similar to profile data as published in Ref. [2] and in Ref. [1] for a 1.7 T DIII-D equilibrium). Two regions of power absorption are found by the calculation: the first is the region at  $\rho \gtrsim 0.4$ , which, accounting for the flux surface volumes, represents approximately 50% of the launched power which is absorbed from the X mode on the first pass through the cyclotron resonance, while the inner region is due to the Doppler shifted absorption of the EBW and is significantly nearer to the plasma centre. The EBW power is absorbed in a smaller volume and so the power density is larger.

The  $N_\parallel$  upshift is a geometric effect resulting from variations of  $B$  within a flux surface, curvature and magnetic shear. As such, it is influenced by the poloidal magnetic field of the tokamak. This can be understood from ray tracing Eqs (2) by

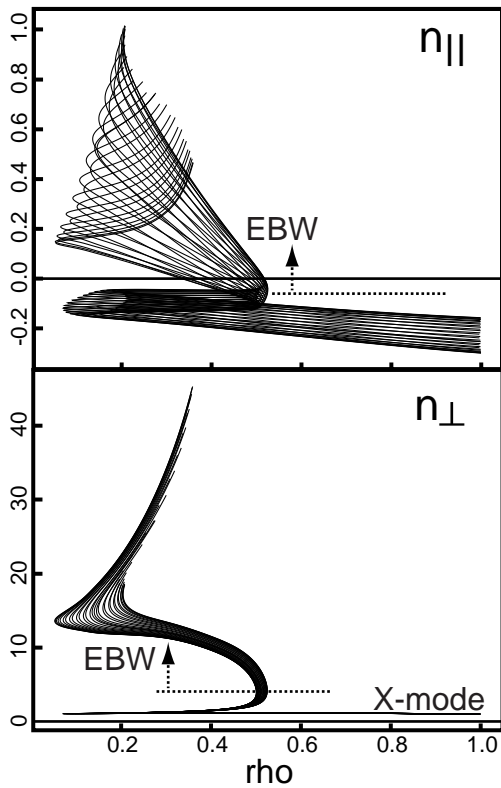


**Figure 3.** Variations of  $N_{\perp}$  and  $N_{\parallel}$  along the launched rays shown in Fig. 1.

evaluating the  $N_{\parallel}$  evolution. Since density and temperature are constant on a flux surface and the equilibrium is independent of toroidal angle,

$$\frac{dN_{\parallel}}{dt} = \frac{c}{\omega} \frac{\partial D / \partial B}{\partial D / \partial \omega} \frac{\mathbf{B}_p}{B} \cdot \nabla B - \left( V_{g,\parallel} - \frac{N_{\parallel}}{N_{\perp}} V_{g,\perp} \right) \times \mathbf{N} \cdot (\hat{\mathbf{b}} \cdot \nabla) \hat{\mathbf{b}} + \frac{V_{g,\perp}}{N_{\perp}} \mathbf{N} \cdot (\mathbf{N} \cdot \nabla) \hat{\mathbf{b}} \quad (5)$$

Each of the terms on the right hand side of Eq. (5) contributes to the  $N_{\parallel}$  shift. The first term on the right hand side is due to variation of the magnetic field within a flux surface and is proportional to the strength of the poloidal field. In these calculations, the launched power is represented by 30 rays to model the  $N_{\parallel}$  spectrum of the launching horn. Figure 3 shows the  $N_{\parallel}$  and  $N_{\perp}$  along the ray trajectories.

This upshift has already been noted [6], and in particular the  $N_{\parallel}$  variation is expected to be strongly affected by the poloidal launch position of the EBW relative to the midplane. Similar results have also been found in simulations of the propagation of the ion Bernstein wave [8, 9]. The DIII-D antenna is located 10 cm above the midplane, and would therefore be well suited for launching waves which undergo

$N_{\parallel}$  upshift. Sensitivity studies (with respect to equilibrium, temperature and density) show that the width and location of the EBW deposition can vary by several centimetres, but that the results are robust in providing more central deposition with respect to variation in temperature.

We emphasize that the ray tracing and power deposition of the EBW as computed here should be considered to be the theoretically expected power deposition profile, where the EBW is absorbed before it is able to propagate back to the cyclotron resonance layer. The calculations presented here predict more central power deposition than was estimated in the DIII-D experiments, where it was attributed to transport. The power deposition was estimated experimentally using two techniques. The first was an Abel inversion of the changing soft X ray emission during ECH turn-on (shown in Fig. 2 of Ref. [2]) which had a spatial resolution of 6 cm. This measurement showed more central deposition than predicted by an absorption calculation without inclusion of the EBW, but not as strong a deposition as predicted here. The authors dismiss the profiles as artefacts of the inversion technique; given the ill posed nature of the inversion process, we note that the inverted profile as presented must at least be mathematically consistent with the data. It is our interpretation that the inverted profile is not an unreasonable estimate of the deposition profile (we note that Abel inversion of hollow profiles, in this case with two closely located peaks, is very difficult to model and requires better spatial resolution than present on DIII-D at the time). The second technique was to follow the time evolution of  $T_e$  measured by Thomson scattering immediately following turn-on; this also shows deposition more centrally peaked than the cold plasma cyclotron resonance position would predict, although not as central as the EBW predicts.

Several possibilities exist for explaining the reduced experimentally measured deposition relative to the calculation. First, non-linear effects giving parametric instabilities near the upper hybrid resonance (the mode conversion region) and along the EBW ray are not considered. Experiments on Versator with a similar high field side launch observed parametric decay of the X mode into the EBW and a lower hybrid wave [10]. It is conjectured that the parametric decay would lead to a change in the  $N_{\parallel}$  of the EBW and would lead to a larger Doppler shift in the resonance position; this shift would broaden the EBW deposition. Indeed, plasma formation experiments on TCA with high field side launch X mode

showed that a majority of the power was absorbed at the upper hybrid layer [11]. Wave absorption closer to the upper hybrid layer would be sufficient for reconciliation with the turn-on measurements mentioned above, since the upper hybrid layer coincides with the same flux surface as the cold resonance layer (but on the low field side of the magnetic axis). These effects are related to, but beyond the scope of, the linear ray tracing theory we have presented here, since they involve scattering of the mode converted EBW. Secondly, the role of transport has not been considered here. The absorption is dependent upon the  $q$  profile and upon the temperature (although weakly), and the transient response can be modified by the nature of the transport. These are questions for future experiments to address.

In summary, proper accounting of the mode converted EBW in the DIII-D heat pinch experiments explains part of the discrepancies of the power balance analysis which led to the idea of a heat pinch. For the DIII-D experiment, the X mode is expected to be mode converted to the EBW, the  $N_{\parallel}$  of the EBW is expected to be upshifted in magnitude, and substantial power deposition is expected to be shifted from the resonance layer towards the centre of the discharge. Non-linear effects such as parametric decay, which are beyond the scope of this study, may lead to absorption on the upper hybrid resonance layer or more central deposition. Here we have studied the ray propagation and absorption in a discharge similar to that reported in Ref. [2]; future studies could include more detailed comparison with a variety of shots, but the results are expected to be robust. We have not performed a power balance analysis although estimates indicate that the central absorption is sufficient to give an outward heat flux over a much larger region of the plasma. The EBW calculations shown here do not predict power deposition in the immediate vicinity of the magnetic axis (for  $\rho < 0.15$ ); thus our conclusions do not rule out the possibility of a heat pinch in this region. Discrepancies between the power deposition calculations and the power deposition measurements exist; however, there is also a discrepancy between these measurements and the original power deposition calculation used to infer the heat pinch. If the experimentally determined power deposition profiles were to be used in the original paper, our conclusions

would still be supported. Finally, we note that other ECH scenarios, such as outside launch scenarios and second harmonic scenarios, would not be expected to have central EBW heating. This is consistent with the failure of other attempts to observe the heat pinch on other devices using different ECH geometries. In particular, in off-axis ECH experiments both on the ASDEX-Upgrade tokamak [12] and on the RTP tokamak [13] it has been concluded that there is no evidence for a heat pinch.

## Acknowledgements

One of the authors (CBF) is grateful for discussions with J.D. Callen, S.C. Prager and P.W. Terry, and for helpful suggestions from Referee B which have significantly improved the manuscript. This work is supported by the US Department of Energy.

## References

- [1] Luce, T.C., Petty, C.C., De Haas, J.C.M., Phys. Rev. Lett. **68** (1992) 52.
- [2] Petty, C.C., Luce, T.C., Nucl. Fusion **34** (1994) 121.
- [3] Bornatici, M., Cano, R., De Barbieri, O., Engelmann, F., Nucl. Fusion **23** (1983) 1153.
- [4] Stix, T.H., Phys. Rev. Lett. **15** (1965) 878.
- [5] Schuss, J., Hosea, J., Phys. Fluids **18** (1975) 727.
- [6] Forest, C.B., Chattopadhyay, P.K., Harvey, R.W., Smirnov, A.P., Phys. Plasmas **7** (2000) 1352.
- [7] Stix, T.H., Waves in Plasmas, American Inst. of Physics, New York (1992).
- [8] Ram, A., Bers, A., Phys. Fluids B **3** (1991) 1059.
- [9] Ono, M., Phys. Fluids B **5** (1993) 241.
- [10] McDermott, F., Bekefi, G., Hackett, K., Levine, J., Porkolab, M., Phys. Fluids **25** (1982) 1488.
- [11] Whaley, D.R., Nucl. Fusion **32** (1992) 757.
- [12] Gruber, O., et al., Nucl. Fusion **39** (1999) 1321.
- [13] De Baar, M., Beurskens, M., Hogeweij, G., Cardozo, N.L., Phys. Plasmas **6** (1999) 4645.

(Manuscript received 15 December 2000

Final manuscript accepted 15 February 2001)

E-mail address of C.B. Forest:  
cbforest@facstaff.wisc.edu

Subject classification: F1, Te; G1, Te